Laser and Particle Beams (2013), *31*, 547–550.

doi:10.1017/S026303461300058X

Generation of periodic structures on SiC upon laser plasma XUV/NIR radiations

L. GEMINI,[1] D. MARGARONE,[2] S. TRUSSO,[3] L. JUHA,[4] J. LIMPOUCH,[1,2] T. MOCEK,[5] AND P.M. OSSI[6]

[1]FNSPE, Czech Technical University in Prague, Prague, Czech Republic
[2]ELI Beamlines Project, Institute of Physics of the ASCR, Prague, Czech Republic
[3]CNR-IPCF, Istituto per i Processi Chimico-Fisici, Messina, Italy
[4]Institute of Physics of the ASCR, Prague, Czech Republic
[5]HiLASE Project, Institute of Physics of the ASCR,, Czech Republic
[6]Dip. Energia, Politecnico di Milano, Milano, Italy

(Received 6 May 2013; Accepted 3 June 2013)

Abstract

Surface periodic structures are generated upon irradiation of a silicon carbide (SiC) thin film by the plasma produced by 40 fs pulses from a Ti:Sapphire laser focused onto a thick low density polyethylene (LDPE) foil facing the SiC film. Independently of the number of laser pulses applied, these structures, with average regular periodicity of 710 nm, are evident throughout all irradiated areas. We attribute their formation to the efficient coupling of the unfocused femtosecond laser pulse with the incoherent extreme ultraviolet component of the laser-generated LDPE plasma.

Keywords: Generation of periodic structures; Laser plasma irradiation of SiC; LDPE plasma formation by ultra-short pulse laser; XUV/NIR dual action

1. INTRODUCTION

Femtosecond lasers provide unique possibilities for high-precision material processing: thanks to its very fast interaction process, the heat affected zones in the irradiated targets are strongly localized, with minimal residual damage (Gottmann *et al.*, 2008; Boulmer-Leborgne *et al.*, 2010). In this framework, the generation of laser induced periodic surface structures (LIPSS) from femtosecond pulse direct irradiation has been intensively studied on various materials, including metals, insulators, and semiconductors (Tomita *et al.*, 2008; Reif *et al.*, 2008; Okamuro *et al.*, 2010). Among the latter, silicon carbide (SiC) has proved to be a very promising material with high performances in different application fields, as for instance MEMS fabrication and solar cell development (Yu *et al.*, 2012; Winkler *et al.*, 2012; Pecholt *et al.*, 2011; 2008). Although different models have been proposed to explain the generation of periodic self-forming structures in the femtosecond regime of irradiation, the complete process of their generation is still debated (Reif *et al.*, 2011; Bonse *et al.*, 2011; Derrien *et al.*, 2012; Sakabe *et al.*, 2009). Recently, using a complex experimental setup, femtosecond near-infrared (NIR) laser pulses were applied to amorphous Carbon (a-C) films together with an extreme ultraviolet (XUV) beam. Under such conditions, although the fluence was kept below the ablation threshold of a-C in all irradiation geometries, a significant increase of both the spatial periodicity and the peak-to-valley depth of LIPSS were observed over that from NIR irradiation alone. LIPSS enhancement was attributed to the combined XUV-NIR action (Mocek *et al.*, 2012).

In this paper, we are not reporting on LIPSS formation as usually meant. Instead, we demonstrate that extended periodic structures can be generated on a SiC surface by irradiation from plasma produced by 40 fs laser pulses.

2. EXPERIMENTS

A SiC film about 130 nm thick was deposited by a pulsed laser onto a Si (100) substrate kept at 1173 K using a KrF excimer laser (wavelength 248 nm, pulse duration 25 ns, fluence 6 J cm^{-2}). A homogeneous, compact film, free from surface particulate was obtained. A Ti:Sapphire laser (wavelength 800 nm, pulse width 40 fs, electric field polarization inclined at 6° with respect to the normal incidence direction)

Address correspondence and reprint requests to: L. Gemini, FNSPE, Czech Technical University in Prague, Brehova 7, 11519, Prague, Czech Republic. E-mail: gemini@fzu.cz

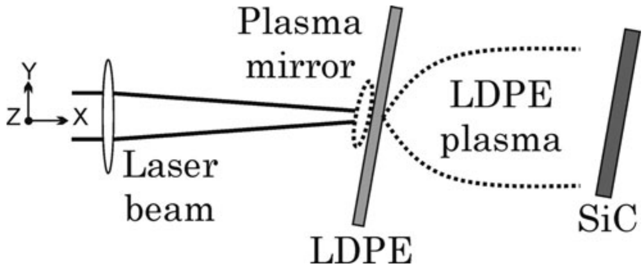

Fig. 1. Schematic of the experimental setup (top view) and of the main physical processes which occur during the interaction between the laser beam and the LDPE foil (generation of plasma mirror on the front side and LDPE plasma expansion on the rear side of the foil).

was focused on a 15 μm thick low density polyethylene (LDPE) film, directly facing the SiC film at a distance of about 1 cm (Fig. 1). Each laser pulse, with an intensity on the order of 10^{18} Wcm^{-2}, impinged on the LDPE inclined at 10° with respect to the target normal. Due to the presence of a laser pulse nanosecond pedestal with intensity on the order of 10^{12} Wcm^{-2}, the laser-irradiated LDPE was partially converted into a plasma carrying fast C and H ions and generating incoherent XUV photons, which expanded and irradiated the SiC film. The LDPE foil was mounted on a motorized YZ so that each laser pulse produced an LDPE plasma pulse. This way every single laser pulse generated an identical LDPE plasma pulse irradiating its associated SiC sample area.

A 15 μm thick Mylar foil was laser irradiated under the same experimental conditions described for the LDPE irradiation. Ion time-of-flight (TOF) spectra (Fig. 2) referred to the plasma generated during Mylar irradiation on the rear side of the target were collected by a Faraday cup and by a fast response SiC detector to evaluate the low energy and the high energy ion components, respectively (Margarone

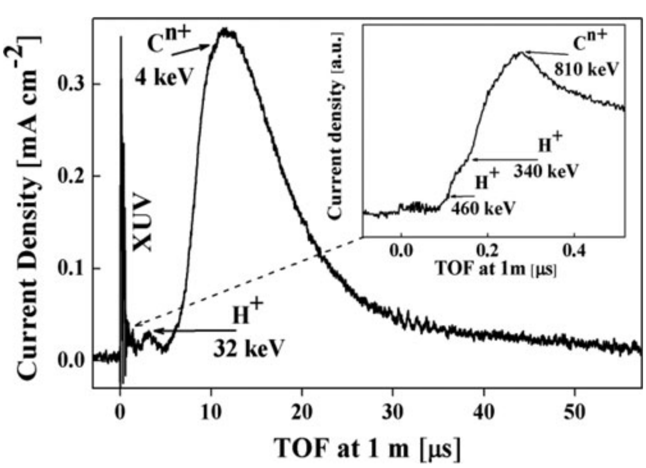

Fig. 2. TOF spectra referring to plasma generated during irradiation of a 15 μm Mylar foil, collected by a Faraday cup (PIC) and a SiC detector (inset). It is noteworthy that the high energy component intensity collected by the SiC detector (inset) is negligible, being far below that of the low energy component.

et al., 2011). For our purposes, the features of this spectrum can be considered analogous to those obtained from the LDPE-generated plasma. The TOF signals show the presence of an XUV photo-peak followed by H^+ and C^{n+} signals (after several microseconds) peaked at the energies of 32 and 4 keV, respectively. A proton maximum energy approaching 500 keV, and H^+ and C^{n+} peak energies of 340 and 810 keV were measured by a fast response SiC detector for proton and carbon ions, respectively. The slow and the fast ion components can be associated to the nanosecond laser generated plasma (due to the laser pedestal) and to the femtosecond laser interaction, respectively.

It is important to observe that the XUV photo-peak impinges on the sample surface much earlier than the low energy ion component and right before the high energy ion component, whose estimated number density is anyway negligible (about 1% of the total ion contribution). Therefore the SiC surface is first irradiated by the XUV component together with the 40-fs NIR laser beam, the intensity of the latter being reduced to about $8{\cdot}10^{11}$ Wcm^{-2} due to the unfocusing condition, the LDPE absorption, the plasma mirror effect induced on the front side of the LDPE target, and the absorption by the expanding LDPE plasma on the rear side of the LDPE target (the estimated transmitted NIR beam that irradiates the sample surface after all the above mentioned processes is indeed less than 1%).

3. RESULTS AND DISCUSSION

Different areas of the SiC sample were irradiated by a different number of LDPE plasma pulses, from 1 to 5, to observe the effects of the progressively cumulating plasma pulses on the SiC. Every irradiation produced a circularly shaped modification on the sample surface with a diameter of about 4 mm. For comparison, a reference SiC area was irradiated by five pulses of the unfocused femtosecond beam in the absence of LDPE. All the irradiated areas were analyzed by a scanning electron microscope (SEM Zeiss Supra 40 field ion instrument). Since the estimated NIR fluence at the sample surface (about 32 $mJcm^{-2}$) was well below the ripple generation threshold of SiC in the femtosecond regime, the surface irradiated by unfocused femtosecond pulses in the absence of LDPE plasma appears unchanged with respect to the as-deposited material, as shown in Figure 3 (Dong & Molian, 2003). Independently of the number of laser pulses, a wavy surface morphology is visible in all the areas irradiated by LDPE plasma pulses as shown in Figure 4: such ripples are most evident in the area irradiated by a single plasma pulse, and they lose definition with increasing pulse number. Energy dispersive X-ray spectroscopy (EDX, by SEM) indicates that all the plasma irradiated areas consist of SiC. It is noteworthy that the wavy structure extends across the entire areas irradiated by the laser induced plasma, without being limited to the center of a laser spot: indeed no laser spots are produced on the SiC surface, due to the indirect irradiation conditions.

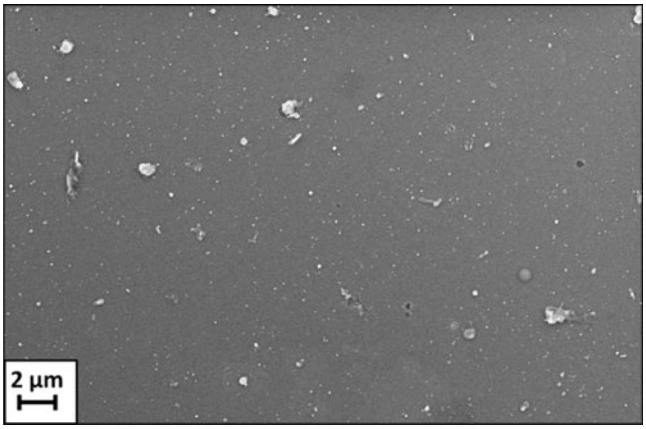

Fig. 3. SiC surface irradiated by unfocused NIR light alone. The surface appears unmodified compared to the as deposited material.

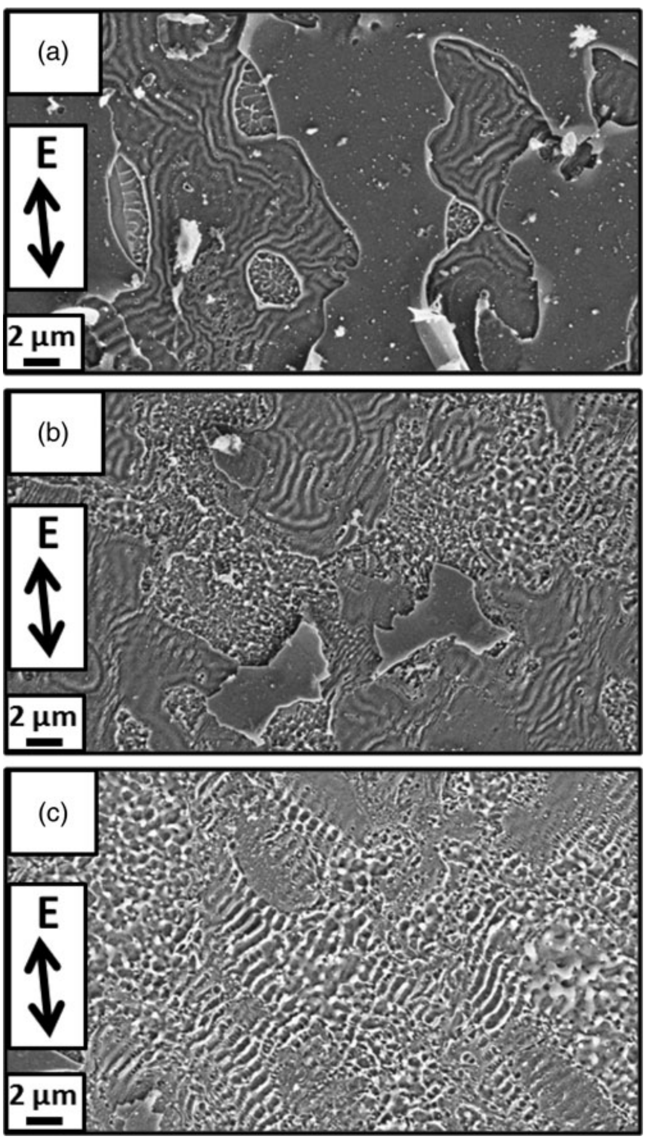

Fig. 4. SEM images of the areas irradiated by LDPE plasma generated by single pulse (**a**), three pulses (**b**) and five pulses (**c**). The arrows indicate the direction of the laser electric field E polarization.

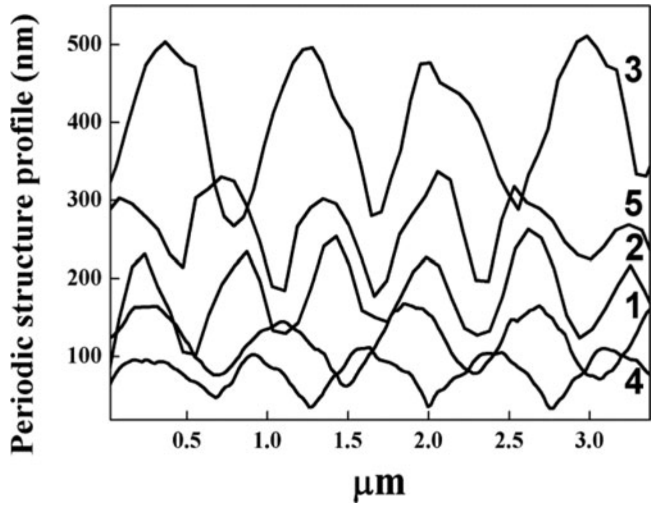

Fig. 5. AFM periodic structure profiles of areas irradiated by LDPE plasma generated by 1 to 5 laser pulses. The numbers on the right side indicate the laser pulse number.

All modified areas were analyzed by an atomic force microscope (AFM Bruker Dimension Icon with ScanAsyst and AFM Ntegra Prima, both working in tapping mode in air). The AFM measurements were affected by the presence of dust and impurities on the sample surface. We preferred not to clean the sample in order to avoid possible surface contamination and alteration.

Representative profiles of the analyzed areas are shown in Figure 5. Independently of the number of laser pulses, the AFM profiles show that the wavy structure is characterized by a periodicity ranging from 638 nm to 826 nm with an average value of 710 nm, slightly smaller than the laser wavelength, and by a peak-to-valley depth ranging from 70 nm to 219 nm, leading to an average value of 123 nm. Every area, as related to a definite number of plasma pulses, is characterized by a specific, constant value of peak-to-valley depth and by a constant spatial periodicity.

On the basis of these results, the formation of plasma induced ripples is likely to be associated to the coupling of the unfocused femtosecond laser beam with the incoherent XUV component of the laser-produced LDPE plasma. The experimental results may be explained in terms of a simplified physical picture. The strong coupling between the NIR laser beam and the XUV/NIR-irradiated solid is attributed to efficient free electron generation via linear absorption of highly energetic XUV photons. Such clouds of free electrons undergo free-carrier absorption of NIR light, in turn leading to an increase in the absorption coefficient of optical radiation and consequently to a fast, strong increase of both temperature and pressure in the near-surface region of the illuminated material (Bulgakova *et al.*, 2010). The resulting highly unstable state relaxes via material melting and convective mass transport can then be taken into account (Siwick *et al.*, 2003; Ravindran *et al.*, 2004). The interference between waves scattered by defects in the material and the

https://doi.org/10.1017/S026303461300058X Published online by Cambridge University Press

incident beam produces a spatial modulation of the light intensity in the molten material which leads to a consequent spatial modulation of the pressure, where the crests correspond to sites with higher enthalpy, intensity and pressure. In such a liquid material, a collective behavior in the form of convection currents arises and causes the transport of mass into the areas where the intensity, i.e., the pressure, is higher, ultimately leading to the generation of a periodic surface structure. Thus the formation of rippled structures corresponds to an efficient relaxation of local tension at the material surface. Nevertheless more detailed experiments are planned to validate the proposed model and to investigate the phenomena that take place during the interaction between the LDPE plasma and the SiC surface.

4. CONCLUSIONS

In summary, we have shown that the irradiation of a SiC surface with femtosecond laser-generated LDPE plasma leads to an efficient generation of periodic structures: such nanostructures grow over the entire area irradiated by the plasma, regardless of the propagation direction of the laser beam, only when the laser beam is coupled with an incoherent XUV source. We attribute the generation of these ripples to the effect of the dual action of the unfocused femtosecond laser beam with the incoherent XUV component of the laser-generated LDPE plasma. It is remarkable that the incoherent XUV radiation is here obtained directly from the plasma, removing the need for a directional XUV source such as high-order harmonics (Mocek *et al.*, 2012). This fact, together with the use of a NIR beam out from the focus position, permits obtaining an enhanced generation of a periodic surface structure with a very simple experimental setup. Remarkably, the surface areas affected by the highly repetitive self-organized periodic structuring are broad, homogeneous, and extend over regions of about 2 mm^2 each, thus opening the way to large-scale applications of this surface treatment.

ACKNOWLEDGEMENTS

This work benefitted from the support of the Czech Science Foundation (Project P205/11/1165), the Czech Republic's Ministry of Education, Youth and Sports support of the HiLASE (CZ.1.05/2.1.00/01.0027), the ELI-Beamlines (CZ.1.05/1.1.00/ 483/02.0061), and the OPVK (CZ.1.07/2.3.00/20.0087) projects, and the Czech Technical University in Prague (RVO68407700).

REFERENCES

Bonse, J., Rosenfeld, A. & Kruger, J. (2011). Implications of transient changes of optical and surface properties of solids during femtosecond laser pulse irradiation to the formation of laser-induced periodic surface structures. *Appl. Surf. Sci.* **257**, 5420.

Boulmer-Leborgne, C., Benzerga, R. & Perriere, J. (2010). Nanoparticle formation by femtosecond laser ablation. In *Laser-Surface Interactions for New Material Production* (Miotello, A. & Ossi, P.M, Eds.) Berling: Springer-Verlag, p. 125.

Bulgakova, N., Stoian, R., Rosenfeld, A. & Hertel, I.V. (2010). Continuum Models of Ultrashort Pulsed Laser Ablation. In *Laser-Surface Interactions for New Material Production* (Miotello, A. & Ossi, P.M., Eds.). Berlin: Springer-Verlag, p. 82.

Derrien, T.J.-Y., Torres, R., Sarnet, T., Sentis, M. & Itina, T.E. (2012). Formation of femtosecond laser induced surface structures on silicon: Insights from numerical modeling and single pulse experiments. *Appl. Surf. Sci.* **258**, 9487.

Dong, Y. & Molian, P. (2003). Femtosecond pulsed laser ablation of 3C-SiC thin film on silicon. *Appl. Phys. A* **77**, 839.

Gottmann, J., Wortmann, D. & Wagner, R. (2008). Manufacturing of periodical nanostructures by fs-laser direct writing. *Proc. SPIE* **7022**, 702202.

Margarone, D., Krása, J., Giuffrida, L., Picciotto, A., Torrisi, L., Nowak, T., Musemeci, P., Velyhan, A., Prokůpek, J., Láska, L., Mocek, T., Ullschmied, J. & Rus, B. (2011). Full characterization of laser-accelerated ion beams using Faraday cup, silicon carbide, and single-crystal diamond detectors. *J. Appl. Phys.* **109**, 103302.

Mocek, T., Jakubczak, K., Chalupsky, J., Park, S.B., Lee, G.H., Kim, T.K., Nam, C.H., Hajkova, V., Toufarova, M., Gemini, L., Margarone, D., Juha, L. & Rus, B. (2012). Efficient surface processing by ultrafast XUV/NIR dual action. *Proc. SPIE* **8206**, 82061H.

Okamuro, K., Hashida, M., Miyasaka, Y., Ikuta, Y., Tokita, S. & Sakabe, S. (2010). Laser fluence dependence of periodic grating structures formed on metal surfaces under femtosecond laser pulse irradiation. *Phys. Rev. B* **82**, 165417.

Pecholt, B., Gupta, S. & Molian, P. (2011). Review of laser microscale processing of silicon carbide. *J. Laser Appl.* **23**, 012008.

Pecholt, B., Vendan, M., Dong, Y. & Molian, P. (2008). Ultrafast laser micromachining of 3C-SiC thin films for MEMS device fabrication. *Int. J. Adv. Manuf. Technol.* **39**, 239.

Ravindran, K., Srinivasan, J. & Marathe, A.G. (2004). Finite element study on the role of convection in laser surface melting. *Numer. Heat Trans. A* **26**, 601.

Reif, J., Varlamova, O. & Costache, F. (2008). Femtosecond laser induced nanostructure formation: self-organization control parameters. *Appl. Phys. A: Mater. Sci. Process*. **92**, 1019.

Reif, J., Varlamova, O., Varlamov, S. & Bestehorn, M. (2011). The role of asymmetric excitation in self-organized nanostructure formation upon femtosecond laser ablation. *Appl. Phys. A: Mater. Sci. Process*. **104**, 969.

Sakabe, S., Hashida, M., Tokita, S., Namba, S. & Okamuro, K. (2009). Mechanism for self-formation of periodic grating structures on a metal surface by a femtosecond laser pulse. *Phys. Rev. B* **79**, 033409.

Siwick, B.J., Dwyer, J.R., Jordan, R.E. & Miller, R.J.D. (2003). An Atomic-Level View of Melting Using Femtosecond Electron Diffraction. *Sci.* **302**, 1382.

Tomita, T., Fukumori, Y., Kinoshita, K., Matsuo, S. & Hashimoto, S. (2008). Observation of laser-induced surface waves on flat silicon surface. *Appl. Phys. Lett.* **92**, 013104.

Winkler, M.T., Sher, M.-J., Lin, Y.-T., Smith, M.J., Zhang, H., Gradečak, S. & Mazur, E. (2012). Studying femtosecond-laser hyperdoping by controlling surface morphology. *J. Appl. Phys.* **111**, 093511.

Yu, J.S., Leem, J.W., Ko, Y.H. & Lee, H.K. (2012). Semiconductor nanostructures towards optoelectronic device applications. *Proc. SPIE* **8268**, 82680A.